Highly Asymmetric Lamellar Nanopatterns *via* Block Copolymer Blends Capable of Hydrogen Bonding

Sung Hyun Han,[†] Victor Pryamitsyn,[‡] Dusik Bae,[†] Jongheon Kwak,[†] Venkat Ganesan,[‡,*] and Jin Kon Kim[†,*]

[†]National Creative Research Center for Block Copolymer Self-Assembly, Department of Chemical Engineering, Pohang University of Science and Technology, Kyungbuk 790-784, Korea and [‡]Department of Chemical Engineering, University of Texas, Austin, Texas, United States

ABSTRACT

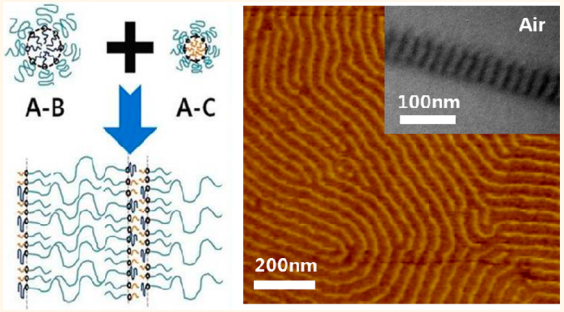

Highly asymmetric lamellar microdomains, such as those required for many lithographic line patterns, cannot be straightforwardly achieved by conventional block copolymer self-assembly. We present a conceptually new and versatile approach to produce highly asymmetric lamellar morphologies by the use of binary blends of block copolymers whose components are capable of hydrogen bonding. We first demonstrate our strategy in bulk systems and complement the experimental results observed by transmission electron microscopy and small-angle X-ray scattering with theoretical calculations based on strong stretching theory to suggest the generality of the strategy. To illustrate the impact on potential lithographic applications, we demonstrate that our strategy can be transferred to thin film morphologies. For this purpose, we used solvent vapor annealing to prepare thin films with vertically oriented asymmetric lamellar patterns that preserve the bulk morphological characteristics. Due to the highly asymmetric lamellar microdomains, the line width is reduced to sub-10 nm scale, while its periodicity is precisely tuned.

KEYWORDS: tunable nanoscopic line patterns · block copolymer lithography · highly asymmetric lamellar microdomains · blend of block copolymers · hydrogen bonding

Manufacturing next-generation storage devices and integrated circuits requires feature sizes less than 20 nm.[1] In this context, lithography based on self-assembly of block copolymers has received significant attention due to the ability to achieve morphologies with dimensions in the range 10−20 nm.[2−16] In conjunction with chemically and physically nanopatterned substrates, epitaxial assembly of the defect-free microdomains of block copolymers over large areas has been demonstrated as a means to achieve lithography targets.[6−16] Typically, the block copolymer microdomains used for this purpose have been based on periodic lamellar morphologies. However, in diblock copolymers, such lamellar morphologies usually arise only in a narrow range of block compositions in which the volume fractions of the two components are approximately the same. Thus, the resulting morphologies have been restricted to symmetric and nearly symmetric widths of the microdomains. However, for the next-generation nanoscopic patterns required in lithography, the above strategies need to be extended to allow for highly asymmetric line patterns (wherein the microdomain width of one of the nanopatterns is significantly different from the other) in nanoscale, similar to those that could be obtained through techniques such as top-down e-beam lithography. Moreover, such strategies should also be versatile enough to achieve microdomains in the sub-20 nm size scales. Unfortunately, however, when the volume fraction of one of the blocks in the block copolymers is much smaller than the other block, spherical and cylindrical microdomains are formed instead of lamellar microdomains.[17] As a consequence, fabrication of asymmetric line patterns based on block copolymer lithography has remained an unfulfilled challenge.

Since the morphologies achievable by a single-component block copolymer system are limited by their average volume fractions and temperature, a potential alternative strategy to address the above challenges would be to use blends of two or more block copolymers. Indeed, some research groups have demonstrated that the self-assembly morphologies could be modified by blending block copolymers with different molecular

* Address correspondence to jkkim@postech.ac.kr, venkat@che.utexas.edu.

Received for review June 7, 2012 and accepted August 20, 2012.

Published online August 20, 2012
10.1021/nn3025089

weights and/or different chemical structures.[18−23] Yet, even within such a framework, to prepare highly asymmetric lamellar microdomains, one is forced to choose highly asymmetric blend compositions in the block copolymers. In such situations, the polymer chain stretching energy costs dominate and lead to the formation of curved morphologies.

In this study, we introduce a conceptually new and versatile strategy to achieve asymmetric line patterns. In a previous study we found that in binary blends of symmetric A−B and A−C diblock copolymers of different molecular weights, specific hydrogen (H−) bonding interactions between the B and C blocks could be used to create body-centered cubic (bcc) spherical microdomains[24] even for nearly compositionally symmetric A−B and A−C diblock copolymers. The results were explained by using self-consistent mean field theory and suggested that the H-bonding interactions between the blocks in a blend may provide a strategy to modify the curvature of the block copolymer microdomains. Here, we demonstrate that blending two compositionally asymmetric block copolymers of appropriate molecular weights with strong H-bonding interactions between the blocks can be used as a strategy to fabricate tunable asymmetric lamellar morphologies with sub-10 nm sizes required for lithographic applications.

RESULTS AND DISCUSSION

Bulk Morphologies. We chose a binary blend of two block copolymers: polystyrene-*b*-poly(2-vinylpyridine) copolymer (PS-*b*-P2VP, denoted as S2VP) and PS-*b*-poly(4-hydroxystyrene) copolymer (PS-*b*-PHS, denoted as SHS). P2VP and PHS exhibit strong interactions arising from H-bonding between N atoms in the P2VP chains and hydroxyl group in the PHS chain.[25] The molecular characteristics and volume fraction of PS block (f_{PS}) in S2VP and SHS are shown in Table 1. Two molecular weights of SHS (SHS-L and SHS-H) were chosen to investigate the effect of the molecular weights on the resulting morphologies.

Both neat S2VP and SHS-H displayed bcc spherical microdomains over the entire range of experimentally probed temperatures. Moreover, SHS-L, which corresponds to a lower molecular weight, also shows bcc spherical microdomain morphologies over the entire range of experimental temperatures (up to 300 °C). This is a consequence of the very large Flory−Huggins segmental interaction parameter ($\chi \approx 0.68$) between PS and PHS.[26] (See section 1 of Supporting Information for the synthesis, characterization, and small-angle X-ray (SAXS) profiles of neat block copolymers.)

Figure 1 presents the main experimental results of this study wherein transmission electron microscopy (TEM) images and SAXS profiles are presented for 80/20 (w/w) S2VP/SHS-L, 50/50 (w/w) S2VP/SHS-H, and 20/80 (w/w) S2VP/SHS-H blends. The SAXS profiles of the blends show the peaks at positions 1:2:3:4, suggesting that all the blends have lamellar microdomains, which is consistent with TEM images. The P2VP and PHS domains appear dark and the PS domains are bright in TEM images because of selective staining by I_2. More pertinently, the width (or size) of PS microdomain (bright region) is seen to be much larger (∼4 times) than that of the (P2VP+PHS) microdomain (dark region).

TABLE 1. Molecular Characteristics and Compositions of Asymmetric PS-*b*-P2VP and PS-*b*-PHSs

PS-*b*-P2VP	M_n (g/mol)[a]	M_w/M_n	f_{PS}	f_{P2VP}
S2VP	106 000	1.07	0.83	0.17
PS-*b*-PHS	**M_n (g/mol)**	**M_w/M_n**	**f_{PS}**	**f_{PHS}**
SHS-L	23 000	1.10	0.82	0.18
SHS-H	43 000	1.09	0.82	0.18

[a] M_n and M_w are the number and weight average molecular weights.

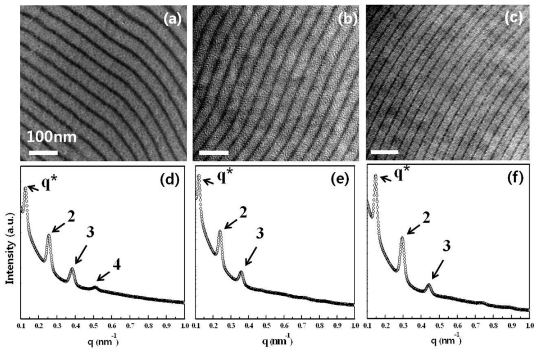

Figure 1. TEM images and SAXS profiles of various blends: (a, d) 80/20 (w/w) S2VP/SHS-L; (b, e) 50/50 (w/w) S2VP/SHS-H; (c, f) 20/80 (w/w) S2VP/SHS-H.

We further analyzed the measured SAXS profiles by fitting with an ideal two-phase lamellar structure model and a variable lamellar thickness model[27] (see Figures S4 and S5 in the Supporting Information). The estimated PS volume fractions in the blends are 0.81−0.86, which is consistent with the f_{PS} of S2VP and SHS used in this study. Furthermore, since the width (or size) of each lamellar microdomain depends only on the volume fraction of the corresponding block, the width ratio of PS to (P2VP+PHS) lamellar microdomains is estimated to be ∼4.5, which is consistent with TEM images in Figure 1 and the enlarged TEM image shown in Figure S6 in the Supporting Information.

Discussion and Theoretical Model. When two asymmetric block copolymers having spherical microdomains are mixed (Figure 2a), intuitively, one would expect one of two possible morphologies: (1) spherical microdomains containing both B and C chains (Figure 2b) or (2) macrophase separation between the two block copolymers (Figure 2c). But, counterintuitive to such expectations, in Figure 1

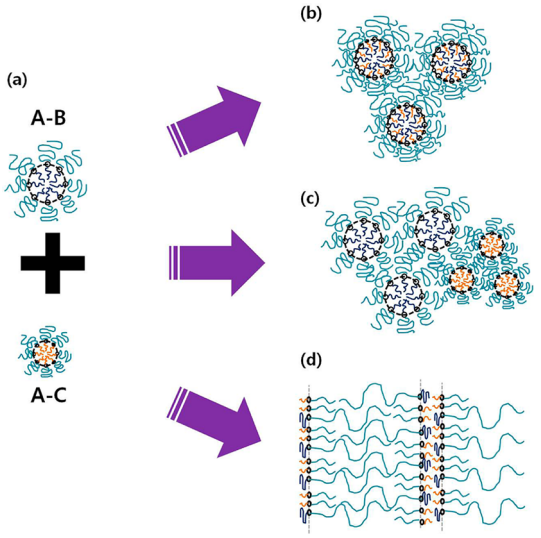

Figure 2. Possible microdomains for binary blends of asymmetric A−B and A−C block copolymers capable of H-bonding between B and C chains.

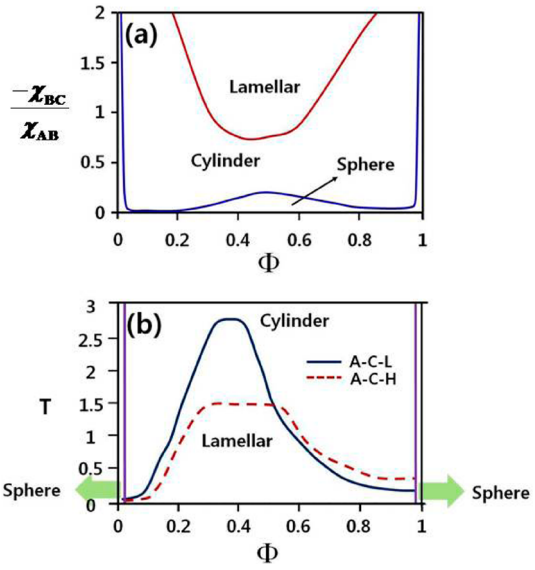

Figure 3. (a) Predicted phase diagram for A−B/A−C binary blend. (b) Predicted phase diagram for A−B/A−C binary blend with two different values of α (0.22 for A−C-L and 0.40 for A−C-H).

we demonstrate the formation of highly asymmetric lamellar microdomains (as shown schematically in Figure 2d), when the minority blocks (B and C) exhibit strong H-bonding interactions.

To elucidate the effect of H-bonding on the phase transformation in the binary blend, we considered a binary mixture of two S2VPs with higher and lower molecular weights (this corresponds to A−B(L) + A−B(H) blend) but the same $f_{PS} = 0.83$. We found that only bcc spherical microdomains were observed without any phase transformation to hexagonally packed (hex) cylinders or lamella (see Figure S7 in the SI) morphologies. This clearly indicates that the difference in molecular weights between the blend components is not the main reason underlying the dramatic changes in interfacial curvature and the morphologies. Thus we infer that the H-bonding interactions play a crucial role in the phase transformation from spherical microdomains into cylindrical and lamellar microdomains.

To explain the unexpected phase transformation observed in this study and explore its generality, we develop a strong stretching theory for S2VP/SHS (denoted as (A−B)/(A−C)) binary blend by adapting Semenov's theory[28] for diblock copolymers. More details of the theoretical framework are presented in the Supporting Information. In brief, we assume that the A, B, and C segments have the same segmental volumes. The molecular weight ratio of A−B and A−C is parametrized by the parameter α. Compositions of the A block in A−B and A−C are defined by parameters f_{AB} and f_{AC}. The volume fraction of the A−C block copolymer in the blend is denoted as Φ. In our theory, the enthalpic interactions are characterized by Flory interaction parameters between A, B, and C segments, for which we assumed $\chi_{AC} = 5\chi_{AB} > 0$ based on the data in the literature.[26,29] While there are known to be H-bonding interactions between P2VP and PHS, a realistic modeling of such interactions is not straightforward within a coarse-grained theory. Consequently, we used a simple model wherein the favorable interaction between P2VP and PHS was modeled by setting the parameter $\chi_{BC} < 0$.

Figure 3a presents the predicted phase diagram for A−B/A−C binary blends with $\alpha = 0.22$ and $f_{AB} = f_{AC} = 0.88$, corresponding to the S2VP/SHS-L blends in the plane of χ_{BC} and Φ. We choose $f = 0.88$, which is slightly larger than the experimental values ($f_{PS} = 0.82-0.83$), because the strong stretching theory (SST) neglects the presence of a finite interfacial width for the microphase-separated domains. Consequently, the transition to bcc microdomains occurs at a slightly larger f compared with the experimental values. In the discussion below, we use the SST results mainly as a tool to shed qualitative light on the physical aspects and the driving forces for the observed morphological transformations.

For the parameters chosen, the neat A−B and A−C block copolymers (corresponding to $\Phi = 0.0$ and 1.0) exhibit bcc spherical morphologies in the SST due to the highly asymmetric volume fractions of the PS block. For A−B/A−C binary blends with relatively weak enthalpic interactions between the B and C blocks, we observe that the bcc spherical morphologies persist regardless of the amount of A−C in the blend. These results are consistent with our experimental observations (see Figure S7 in the SI) in the context of the binary mixture of S2VPs with higher and lower molecular weights (this corresponds to $\chi_{BC} = 0$. in Figure 3). With increasing favorable interactions between B and C, a morphological transformation from bcc spheres

to hex cylinders is observed with increasing content of A−C in the blend. For even stronger interactions between B and C components, which are representative of strong H-bonding interactions, we observe that the cylindrical microdomains are transformed to the lamellar microdomains at intermediate blend compositions, even when the neat block copolymers show bcc spherical morphologies. Moreover, the ratio of the lamellar microdomain width in the blend is predicted to depend only on f_{AB}, and it is given by $f_{AB}/(1 - f_{AB})$. These predictions are consistent with our experimental results and confirm our hypothesis that strong H-bonding interactions can force a transformation of the curved morphologies to noncurved and highly asymmetric lamellar morphologies.

Figure 3b gives the predicted phase diagrams for two values of α ($\alpha = 0.22$ corresponding to A−C-L and $\alpha = 0.4$ to A−C-H) at $\chi_{AC} = 5\chi_{AB} > 0$ and $\chi_{BC}/\chi_{AB} = -2.0$. Here, T is the absolute temperature given by $T = 250/\chi_{AB}N$, in which N is the number of segments in the AB chains. Overall, for both A−C-L and A−C-H blends, there is seen to be a very wide range of A−C content (Φ) over which the blend forms the lamellar microdomains. Interestingly, the A−C-H blend has a wider Φ range compared with the A−C-L blend for the formation of lamellar microdomains. This result is also consistent with our experimental observations in which the 65/35 (w/w) S2VP/SHS-L blend showed hex cylinders consisting of P2VP and PHS chains (see Figure S8 in the SI), whereas the S2VP/SHS-H blend remained in the lamellar morphology up to 90 wt % of SHS-H in the blend (see Figure S9 in the SI). Overall, the theoretical predictions demonstrate that there is a wide region of blending compositions, molecular weight ratios, and temperatures over which the binary blend of block copolymers with intrinsically curved phases can be driven to form highly asymmetric lamellar microdomains.

We now provide a physical explanation of the origin of the above phase transitions, as schematically shown in Figure 4. At low amounts of lower molecular weight A−C in the blend, the A−B chains are expected to be arranged in the bcc spherical microdomains that are bent toward the B and C segments because of the asymmetry in the chain lengths. With increasing amount of A−C, the favorable H-bonding interactions between B and C segments enhance the mixing of B and C segments. This forces the C chains to stretch and B chains to compress. Since nonconcave phases facilitate easier overlap between the B and C components without the concomitant increase in stretching energy penalty, the spherical morphology is transformed to a less concave cylindrical phase and subsequently to the nonconcave lamellar phase.

However, at high amounts of smaller molecular weight A−C-L, the lamellar phase becomes again unstable because the B chains are forced to compress below the unperturbed size of the chains. Then, we

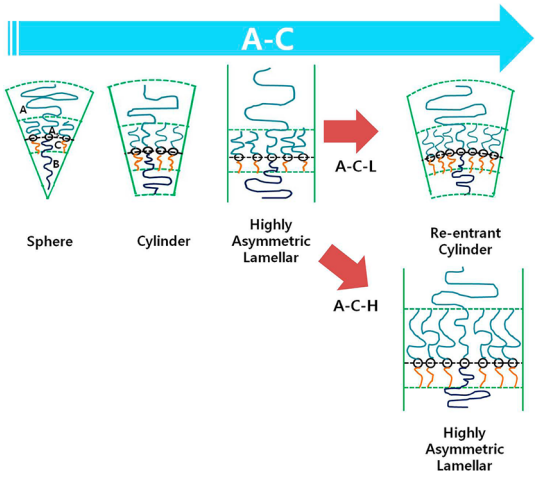

Figure 4. Schematic of phase transitions for asymmetric A−B and A−C block copolymer blends.

observe a re-entrant transition from lamellar microdomains to the cylindrical microdomains. On the other hand, for a binary blend with the higher molecular weight component (A−C-H), since the B chains are not compressed as significantly, lamellar microdomains persist even for higher amounts of A−C-H.

Thin Film Morphologies. To illustrate the potential implications of our strategy for lithographic applications, we demonstrate that the bulk morphologies described in the preceding sections can also be achieved in thin films.

When a film of S2VP/SHS-L blend with a thickness of 158 nm was prepared by spin-coating on a silicon wafer followed by thermal annealing at higher temperature (an extensive discussion of all the experimental details accompanying this section is presented in section S6 in the SI), it displayed parallel orientation of lamellar microdomains with respect to the substrate surface (Figure S11 in the SI). The (P2VP+PHS) chains exhibit favorable interactions with the silicon oxide layer (in the silicon wafer), while the PS chains exhibit lower surface tension compared with the (P2VP+PHS) chains. Thus, the (P2VP+PHS) chains prefer to segregate to the substrate, whereas the PS chains prefer to segregate to the air side. For the asymmetric wetting, which is the case of the thin film of the block copolymer used in this study, parallel orientation of lamellar microdomains is expected when the film thickness (t) satisfies the commensurability condition:[30] $t = (n + (1/2))L_o$, in which L_o is the lamellar domain spacing. Since L_o is 35 nm, as measured in the TEM presented in Figure 1a (thus t is equal to $4.51L_o$), the parallel orientation of highly asymmetric lamellar microdomains observed in Figure S11 is consistent with our expectations.

Lithography applications, however, require that the lamellar microdomains be aligned perpendicularly to the substrate. Although it is not easy to achieve vertically oriented lamellar microdomains for thin films

of highly incompatible block copolymers (such as S2VP or SHS) with asymmetric surface interactions, Russell and co-workers[31] demonstrated a novel strategy to obtain vertically oriented cylindrical P2VP microdomains of S2VP in a thin film with a thickness less than ~30 nm by using a solvent annealing technique. In this work, we adapted the approach given in ref 31 and prepared a *monolayer* of spherical micelles with cores consisting of (P2VP+PHS) chains followed by performing solvent annealing with tetrahydrofuran (THF) vapor. Such a technique allowed us to prepare vertically aligned, highly asymmetric lamellar microdomains in a film with a thickness of ~20 nm, which was confirmed by atomic force microscopy (AFM) (Figure S12 in the Supporting Information).

We note that the approach of ref 31 uses a *monolayer* of spherical micelles and hence allows us to prepare a vertically aligned lamellar microdomain at a very thin film (thickness of ~20 nm). Unfortunately, such films are too thin to verify by cross-sectional TEM imaging whether the asymmetries in line widths observed in bulk samples are indeed preserved. For thicker films (thickness larger than ~40 nm), the method outlined in ref 31 does not allow us to obtain a vertical orientation of lamellar microdomains through the entire film thickness. Thus, we developed a new method that uses multilayered (*not monolayered*) spherical micelles with (P2VP+PHS) to achieve the vertical alignment (see section S6 in the SI for more details) of the asymmetric lamellar microdomains.

Figure 5 shows a phase contrast AFM image and a cross-sectional TEM image of a film with a thickness of ~50 nm prepared by an 80/20 (w/w) S2VP/SHS-L blend after annealing with THF vapor. Highly asymmetric line patterns oriented vertically to the substrate are clearly observed. In the AFM image, the yellow stripes indicate (P2VP+PHS) microdomains, while the brown stripes represent PS microdomains. On the other hand, the dark lines in the TEM image represent (P2VP+PHS) microdomains stained by iodine vapor. The line width of (P2VP+PHS) microdomains was found to be ~7 nm, and that of the PS microdomains was ~28 nm (see also the enlarged AFM and TEM images in Figure S13 in the SI). These two values are seen to be consistent with those in the bulk measured by TEM imaging (Figure 1a). Thus, our bulk morphologies are transferrable to thin films while preserving the asymmetric line patterns.

Since we have already demonstrated through the experiments and theory that the width of the microdomains can be easily tuned by changing the average compositions of the blocks, in combination with the above strategies for thin film processing, our results demonstrate that the width and periodicity of highly asymmetric lines could be precisely controlled to achieve sub-10 nm resolution such as required for development of next-generation lithography.

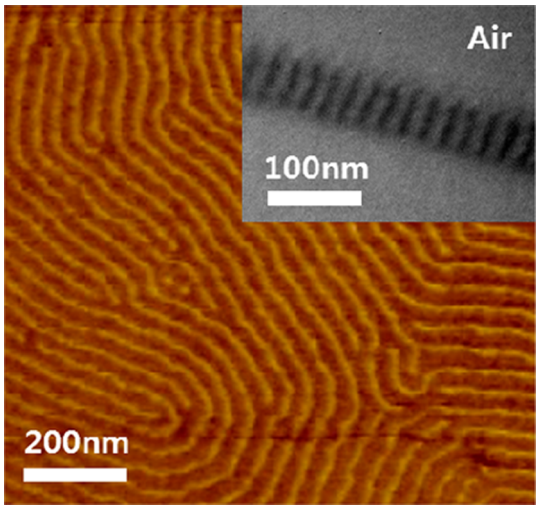

Figure 5. Phase contrast AFM image and TEM image (inset) of a thin film with a thickness of ~50 nm prepared by an 80/20 (w/w) S2VP/SHS-L blend. Vertically oriented asymmetric lamellar microdomains are clearly shown in both images.

It should be noted that the etching contrast between two blocks should be large enough for the application of block copolymer thin films to facilitate lithographic pattern transfer. Unfortunately, such a process cannot be straightforwardly achieved for PS-*b*-P2VP (or PS-*b*-PHS). However, the etching contrast between PS and P2VP (or PHS) can be easily enhanced by overstaining of the P2VP (or PHS) block using iodine because the staining power of P2VP (or PHS) to iodine is much larger than that of PS. Moreover, theoretical calculations indicate that asymmetric line patterns are achievable over a wide range of interaction parameters between A, B, and C blocks.[32] Hence, we are optimistic that our strategy could be expanded to other block copolymers wherein the selective etching of one block is easily achieved. For instance, if the vertical orientation of asymmetric lamellae can be achieved for thin films of a binary blend of polymethylmethacrylate (PMMA)-*b*-P2VP and PMMA-*b*-PHS, the PMMA block can be selectively removed by UV irradiation and rinsing with acetic acid.[3] This is an ongoing research area in our laboratory.

SUMMARY AND CONCLUSIONS

In conclusion, we have demonstrated that the phase behavior of binary blends of block copolymers with strong H-bonding interactions may be used as a versatile approach to fabricate highly asymmetric lamellar microdomains. Through the theoretical and experimental results, we have shown that the H-bonding interactions play a crucial role in the phase transformation from bcc spheres to asymmetric lamellae in the binary blend. Further, we have demonstrated the potential applications by

generating highly asymmetric line patterns oriented vertically on a silicon wafer.

In general, it is very difficult to obtain narrow line widths of less than ~8 nm by using lamellae-forming block copolymers. To achieve this objective, the molecular weight of the block copolymer should be very small, which typically necessitates very low temperatures (or strong incompatibilities between the blocks). Although some research groups have shown that a relatively small line spacing is achieved by using block copolymers having larger χ, for instance, PS-*b*-poly(dimethylsiloxane) copolymers[6] or oligosaccharide-silicon-containing block copolymer,[33] the procedure introduced in our study allows one to generate asymmetric lamellar patterns, which cannot be achieved using such symmetric block copolymers. Moreover, since the asymmetry in the microdomain sizes in our study is mainly determined by the ratio of the volume fraction of the A component relative to the B and C components in the blend, our approach provides easy and versatile control of the asymmetry of the line widths. We also demonstrate that such patterns can be obtained in thin films with perpendicular alignment while preserving the asymmetric line widths observed in bulk morphologies. Hence, this method has the potential to fabricate tunable nanoscopic line patterning for next-generation integrated circuits.

METHODS

Sample Preparation. S2VP was purchased from Polymer Source. Two SHS (SHS-L and SHS-H) were prepared *via* the hydrolysis reaction of PS-*b*-poly(4-*tert*-butoxystyrene) copolymers (PS-*b*-P*t*BOS)s,[34] which were synthesized by the anionic polymerization of styrene and 4-*tert*-butoxystyrene monomers in THF at −78 °C under an argon environment using *sec*-butyllithium (*s*-BuLi) as an initiator. Binary blends with various compositions of S2VP and SHSs were prepared by solution casting using dimethylformamide solvent, followed by slow solvent evaporation at 100 °C, thermal annealing at 180 °C for 5 days under vacuum, and finally quenching to room temperature.

Characterization of the Morphologies. SAXS measurements were performed at room temperature on beamline BL16B1 at the Shanghai Synchrotron Radiation Facility (China), where a double crystal monochromator with two parallel crystals produced monochromatic X-rays on the samples with a wavelength of 0.124 nm and a sample to detector distance of 2 m. A 2-D CCD camera (Princeton Instruments, SCX-TE/CCD-1242) was used to collect the scattered X-rays. The sample was prepared by solution casting, and the thickness was ~400 μm. The X-ray beam was impinged along the sample thickness direction.

Microdomains were observed by using TEM (Hitachi 7600) operating at 100 kV. An ultrathin section of the sample was prepared using a Leica Ultracut Microtome (EM UC6 Leica Ltd.) at room temperature with a thickness of ~40 nm. The section samples were stained with iodine for 2 h at room temperature. Due to the selective staining, PHS and (or) P2VP microdomains look dark in the TEM image.

Highly Asymmetric Line Patterns in a Thin Film Oriented Vertically on the Substrate. A thin film was prepared by spin coating of a 1.5 wt % toluene solution of 80/20 (w/w) S2VP/SHS-L blend at 2000 rpm for 60 s on a silicon wafer with a natural oxide layer and dried under vacuum at room temperature. Because toluene is a selective solvent for PS block,[35] the film morphology was multilayered micelles containing P2VP+PHS cores. The film thickness was ~50 nm. To obtain vertical asymmetric lamellar microdomains, we performed solvent vapor annealing using THF (the details are given in the SI). The surface morphology of the film was observed by scanning force microscopy in the tapping mode (Veeco, DI Dimension 3100 with Nanoscope V), and the cross-sectional image was obtained by TEM (Hitachi 7600). To prepare the sample for TEM, the film was embedded in an epoxy resin after carbon coating, and then the epoxy/carbon/film was removed from the silicon substrate by placing the specimen in liquid nitrogen. Then, the film was microtomed with a Leica Ultracut microtome (EM UC6 Leica Ltd.) at room temperature and stained with iodine vapor.

Conflict of Interest: The authors declare no competing financial interest.

Acknowledgment. This work was supported by the National Creative Research Initiative Program supported by the National Research Foundation (NRF) of Korea. Small-angle X-ray scattering was performed at SSRF (China) and supported by PAL through the abroad beamtime program of Synchrotron Radiation Facility Project under MEST. V.G. and V.P. acknowledge support in part by a grant from the Robert A. Welch Foundation (grant F1599), the U.S. Army Research Office under grant W911NF-10-10346, and National Science Foundation (DMR 1005739).

Supporting Information Available: Synthesis, characterization, and SAXS profiles of neat block copolymers, highly asymmetric lamellar microdomains, morphology of binary blend of higher and lower molecular weight S2VPs, morphologies of 65/35 (w/w) S2VP/SHS-L and 10/90 (w/w) S2VP/SHS-H blends, strong stretching theory for a binary blend of A−B and A−C, and alignment of highly asymmetric microdomains in thin film. These materials are available free of charge *via* the Internet at http://pubs.acs.org.

REFERENCES AND NOTES

1. Kim, H. C.; Park, S. M.; Hinsberg, W. D. Block Copolymer Based Nanostructures: Materials, Processes, and Applications to Electronics. *Chem. Rev.* **2010**, *110*, 146–177.
2. Park, M.; Harrison, C.; Chaikin, P. M.; Register, R. A.; Adamson, D. H. Block Copolymer Lithography: Periodic Arrays of ~10^{11} Holes in 1 Square Centimetre. *Science* **1997**, *276*, 1401–1404.
3. Thurn-Albrecht, T.; Schotter, J.; Kästle, G. A.; Emley, N.; Shibauchi, T.; Krusin-Elbaum, L.; Guarini, K.; Black, C. T.; Tuominen, M. T.; Russell, T. P. Ultrahigh-Density Nanowire Arrays Grown in Self-Assembled Diblock Copolymer Templates. *Science* **2000**, *290*, 2126–2129.
4. Lopes, W. A.; Jaeger, H. M. Hierarchical Self-Assembly of Metal Nanostructures on Diblock Copolymer Scaffolds. *Nature* **2001**, *414*, 735–738.
5. Chai, J.; Wang, D.; Fan, X.; Buriak, J. M. Assembly of Aligned Linear Metalic Patterns on Silicon. *Nat. Nanotechnol.* **2007**, *2*, 500–506.
6. Jung, Y. S.; Chang, J. B.; Verploegen, E.; Berggren, K. K.; Ross, C. A. A Path to Ultranarrow Patterns Using Self-Assembled Lithography. *Nano Lett.* **2010**, *10*, 1000–1005.
7. Kim, S. O.; Solak, H. H.; Stoykovich, M. P.; Ferrier, N. J.; de Pablo, J. J.; Nealey, P. F. Epitaxial Self-Assembly of Block Copolymers on Lithographically Defined Nanopatterned Substrates. *Nature* **2003**, *424*, 411–414.
8. Cheng, J. Y.; Mayes, A. M.; Ross, C. A. Nanostructure Engineering by Templated Self-Assembly of Block Copolymers. *Nat. Mater.* **2004**, *3*, 823–828.
9. Stoykovich, M. P.; Müller, M.; Kim, S. O.; Solak, H. H.; Edwards, E. W.; de Pablo, J. J.; Nealey, P. F. Directed Assembly of Block Copolymer Blends into Nonregular Device-Oriented Structures. *Science* **2005**, *308*, 1442–1446.

10. Han, E.; Leolukman, M.; Kim, M.; Gopalan, P. Resist Free Patterning of Nonpreferential Buffer Layers for Block Copolymer Lithography. *ACS Nano* **2010**, *4*, 6527–6534.
11. Stoykovich, M. P.; Kang, H.; Daoulas, K. C.; Liu, C-. C.; de Pablo, J. J.; Müller, M.; Nealey, P. F. Directed Self-Assembly of Block Copolymers for Nanolithography: Fabrication of Isolated Features and Essential Integrated Circuit Geometries. *ACS Nano* **2007**, *1*, 168–175.
12. Nagpal, U.; Kang, H.; Craig, G. S. W.; Nealey, P. F.; de Pablo, J. J. Pattern Dimensions and Feature Shapes of Ternary Blends of Block Copolymer and Low Molecular Weight Homopolymers Directed To Assemble on Chemically Nanopatterned Surfaces. *ACS Nano* **2011**, *5*, 5673–5682.
13. Bita, I.; Yang, J. K. W.; Jung, Y. S.; Ross, C. A.; Thomas, E. L.; Berggren, K. K. Graphoepitaxy of Self-Assembled Block Copolymers on Two-Dimensional Periodic Patterned Templates. *Science* **2008**, *321*, 939–943.
14. Liu, G.; Thomas, C. S.; Craig, G. S. W.; Nealey, P. F. Integration of Density Multiplication in the Formation of Device-Oriented Structures by Directed Assembly of Block Copolymer-Homopolymer Blends. *Adv. Mater.* **2010**, *20*, 1251–1257.
15. Bosworth, J. K.; Black, C. T.; Ober, C. K. Selective Area Control of Self-Assembled Pattern Architecture Using a Lithographically Patternable Block Copolymer. *ACS Nano* **2009**, *3*, 1761–1766.
16. Son, J. G.; Chang, J-. B.; Berggren, K. K.; Ross, C. A. Assembly of Sub-10-nm Block Copolymer Patterns with Mixed Morphology and Period Using Electron Irradiation and Solvent Annealing. *Nano Lett.* **2011**, *11*, 5079–5084.
17. Matsen, M. W.; Bates, F. S. Unifying Weak- and Strong-Segregation Block Copolymer Theories. *Macromolecules* **1996**, *29*, 1091–1098.
18. Court, F.; Hashimoto, T. Morphological Studies of Binary Mixtures of Block Copolymers. 1. Cosurfactant Effects and Composition Dependence of Morphology. *Macromolecules* **2001**, *34*, 2536–2545.
19. Yamaguchi, D.; Hashimoto, T. A Phase Diagram for the Binary Blends of Nearly Symmetric Diblock Copolymers. 1. Parameter Space of Molecular Weight Ratio and Blend Composition. *Macromolecules* **2001**, *34*, 6495–6505.
20. Chen, F.; Kondo, Y.; Hashimoto, T. Control of Nanostructure in Mixtures of Block Copolymers: Curvature Control *via* Cosurfactant Effects. *Macromolecules* **2007**, *40*, 3714–3723.
21. Asari, T.; Arai, S.; Takano, A.; Matsushita, Y. Archimedean Tiling Structures from ABA/CD Block Copolymer Blends Having Intermolecular Association with Hydrogen Bonding. *Macromolecules* **2006**, *39*, 2232–2237.
22. Valkama, S.; Kosonen, H.; Ruokolainen, J.; Haatainen, T.; Torkkeli, M.; Serimaa, R.; ten Brinke, G.; Ikkala, O. Self-Assembled Polymeric Solid Films with Temperature-Induced Large and Reversible Photonic-Bandgap Switching. *Nat. Mater.* **2004**, *1*, 872–876.
23. Tang, C.; Lenon, C. M.; Fredrickson, G. H.; Kramer, E. J.; Hawker, C. J. Evolution of Block Copolymer Lithography to Highly Ordered Square Arrays. *Science* **2008**, *322*, 429–432.
24. Han, S. H.; Kim, J. K.; Pryamitsyn, V.; Ganesan, V. Phase Behavior of Binary Blends of Block Copolymers Having Hydrogen Bonding. *Macromolecules* **2011**, *44*, 4970–4976.
25. Asari, T.; Matsuo, S.; Takano, A.; Matsushita, Y. Three-Phase Hierarchical Structures from AB/CD Diblock Copolymer Blends with Complementary Hydrogen Bonding Interaction. *Macromolecules* **2005**, *38*, 8811–8815.
26. Zhu, K. J.; Chen, S. F.; Ho, T.; Pearce, E. M.; Kwei, T. K. Miscibility of Copolymer Blends. *Macromolecules* **1990**, *23*, 150–154.
27. Roe, R. J. *Methods of X-ray and Neutron Scattering in Polymer Science*; Oxford University Press, 2000.
28. Semenov, A. N. Contribution to the Theory of Microphase Layering in Block-Copolymer Melts. *Sol. Phys. JETP* **1985**, *61*, 733–742.
29. Zha, W.; Han, C. D.; Lee, D. H.; Han, S. H.; Kim, J. K.; Kang, J. H.; Park, C. Origin of the Difference in Order-Disorder Transition Temperature between Polystyrene-*block*-Poly(2-vinylpyridine) and Polystyrene-*block*-Poly(4-vinylpyridine) Copolymers. *Macromolecules* **2007**, *40*, 2019–2119.
30. Sohn, B. H.; Seo, B. H. Fabrication of the Multilayered Nanostructure of Alternating Polymers and Gold Nanoparticles with Thin Films of Self-Assembling Diblock Copolymers. *Chem. Mar.* **2001**, *13*, 1752–1757.
31. Park, S.; Wang, J-. Y.; Kim, B.; Chen, W.; Russell, T. P. Solvent-Induced Transition from Micelles in Solution to Cylindrical Microdomains in Diblock Copolymer Thin Films. *Macromolecules* **2007**, *40*, 9059–9063.
32. Pryamitsyn, V.; Han, S. H.; Kim, J. K.; Ganesan, V. Curvature Modification of Block Copolymer Microdomains Using Blends of Block Copolymers with Hydrogen Bonding Interactions. *Macromolecules*, under revision.
33. Cushen, J. D.; Otsuka, I.; Bates, C. M.; Halila, S.; Fort, S.; Rochas, C.; Easley, J. A.; Rausch, E. L.; Thio, A.; Borsali, R.; *et al*. Oligosaccharide/Silicon-Containing Block Copolymers with 5 nm Features for Lithographic Applications. *ACS Nano* **2012**, *6*, 3424–3433.
34. Li, M.; Douki, K.; Goto, K.; Li, X.; Coenjarts, C.; Smilgies, D. M.; Ober, C. K. Spatially Controlled Fabrication of Nanoporous Block Coplymers. *Chem. Mar.* **2004**, *23*, 3800–3808.
35. Förster, S.; Antonietti, M. Amphiphilic Block Copolymers in Structure-Controlled Nanomaterial Hybrids. *Adv. Mater.* **1998**, *10*, 195–217.